Jpn. J. Appl. Phys. Vol. 34 (1995) pp. 1778–1783
Part 1, No. 4A, April 1995

Effects of Different Cation and Anion Interdiffusion Rates in Disordered $In_{0.53}Ga_{0.47}As/InP$ Single Quantum Wells

Wai-Chee SHIU, Joseph MICALLEF[1], Isaac NG[2] and E. Herbert LI[2]
Department of Mathematics, Hong Kong Baptist University, Waterloo Road, Hong Kong
[1]*Department of Microelectronics, University of Malta, Msida MSD 06, Malta*
[2]*Department of Electrical & Electronic Engineering, The University of Hong Kong, Pokfulam Road, Hong Kong*

(Received November 7, 1994; accepted for publication January 21, 1995)

The effects of different cation and anion interdiffusion rates when disordering $In_{0.53}Ga_{0.47}As/InP$ single quantum wells are investigated using an error function distribution to model the compositional profile after interdiffusion. The early stages of disordering result in a spatially dependent strain buildup, which can be either compressive or tensile. The effects of this strain profile and the compositional distribution give rise to interesting carrier confinement profiles after disordering. A significantly faster cation interdiffusion rate produces a red shift of the ground-state transition energy, which with prolonged interdiffusion saturates and then decreases. A significantly higher anion interdiffusion rate causes a blue shift in the ground state transition energy, and shifts the light hole ground state above the heavy hole ground state. The results from the model are compared with reported experimental results which have been interpreted in terms of different interdiffusion rates on the two sublattices.

KEYWORDS: InGaAs, quantum well, disordering, strain, confinement profile

1. Introduction

Lattice-matched $In_{0.53}Ga_{0.47}As/InP$ quantum well (QW) structures are of considerable interest in photonic applications, such as waveguides[1] and modulators,[2,3] since they enable device operation in the 1.3 μm to 1.55 μm wavelength range, which is of importance for optical communication systems. Quantum well disordering of III-V semiconductor structures is being actively investigated, with special emphasis on obtaining high-performance device applications and monolithic integration. Selective area disordering of an $In_{0.53}Ga_{0.47}As/InP$ superlattice by argon implantation[4] has been used to modify the fundamental bandgap, and thus the refractive index, in localised areas, resulting in lateral photon confinement in optical waveguides. An impurity-free disordering process has also been used to successfully fabricate polarisation mode selective channel waveguides in an $In_{0.53}Ga_{0.47}As/InP$ disordered superlattice.[5] Selective area disordering of $In_{0.53}Ga_{0.47}As/InP$ QWs, induced by impurity species that are introduced by ion implantation,[6,7] or impurity diffusion,[8–11] or by impurity-free vacancy diffusion,[12] can therefore provide a useful tool for bandgap engineering.

The disordering of $In_{0.53}Ga_{0.47}As/InP$ QW structures is more complicated than the disordering of lattice-matched AlGaAs/GaAs QW structures, or of strained InGaAs/GaAs QWs. Disordering in the latter two structures results in the interdiffusion of only group III atoms,[13,14] while interdiffusion can occur for both group III (In, Ga) and group V (As, P) atoms,[10] in disordered $In_{0.53}Ga_{0.47}As/InP$ QWs. The interdiffusion process in $In_{0.53}Ga_{0.47}As/InP$ QWs is determined by the impurity used to disorder the structure and can result in either a short wavelength[15] or a long wavelength shift[8] in the fundamental absorption edge. The disordered structure may or may not be lattice-matched to InP, so that a strained layer structure may result after interdiffusion.[10]

The disordering of $In_{0.53}Ga_{0.47}As/InP$ QW structures induced by means of various impurity species,[6–11] as well as by impurity-free vacancy diffusion,[12] is being widely investigated experimentally. The results obtained have been interpreted in terms of different interdiffusion processes taking place as a result of the disordering process and the impurity species used. The reported results can be grouped into three interpretations: i) comparable interdiffusion rates on both group III and group V sublattices; ii) cation interdiffusion only; iii) interdiffusion on both sublattices, but with different interdiffusion rates.

Comparable interdiffusion rates on the two sublattices have been proposed to explain the experimental results obtained when considering the disordering of $In_{0.53}Ga_{0.47}As/InP$ QWs induced by sulphur diffusion,[11] by silicon diffusion,[15] as well as by phosphorus-ion implantation.[6] Results of impurity-free compositional disordering by repetitive thermal annealing[12] have also been interpreted to indicate the same extent of interdiffusion on both sublattices. Disordering by Zn diffusion results in a shift of the fundamental absorption edge to longer wavelengths and the experimental results have been interpreted as being due to cation interdiffusion only.[8–10,16] Experimental results on the effects of Ga implantation and subsequent annealing have been interpreted in terms of different interdiffusion rates on the two sublattices.[7]

The effects of interdiffusion on the confinement profile and subband edge structure of an undoped $In_{0.53}GA0.47As/InP$ single QW when the disordering corresponds to cases (i) and (ii) above have been modeled and the results reported elsewhere.[17,18] In this paper, the results of modeling the effects of different interdiffusion rates on the group III and group V sublattices, case (iii) above, on the confinement profile and the subband edge structure are presented and discussed. An error function distribution is used to model the compositional profiles that result after disordering[19] and the effects of strain on the bandgap profile that

results after interdiffusion are taken into consideration to obtain the carrier confinement profiles. This paper is organised as follows: the theoretical basis for the model used in obtaining the compositional distibution, induced strain, carrier confinement potential and subband edge structure of the disordered QW is detailed in §2. The results obtained from the model are then presented and discussed in §3. These results are compared with reported experimental data. Section 4 summarizes the main conclusions of this paper.

2. Model Computations

It is assumed that the group III and group V interdiffusion processes can be modeled by two different diffusion lengths.[7] The interdiffusion of In and Ga atoms is characterized by a diffusion length L_d, which is defined as $L_d=(Dt)^{1/2}$, where D is the diffusion coefficient and t is the diffusion time; the interdiffusion of As and P atoms is characterized by a different diffusion length L_d'. Lattice-matching to InP only exists for $In_xGa_{1-x}As_yP_{1-y}$ materials with $y\approx 2.2(1-x)$,[20] so that the same degree of interdiffusion on both group III and group V sublattices is required to maintain the lattice-matched condition. An interdiffusion process involving only one sublattice,[10] or where the rate of interdiffusion on the group III and group V sublattices differs considerably,[7] will result in a strained material system. If the rates of interdiffusion on group III and group V sublattices are identical, then $L_d'=L_d$ and the lattice-matched condition is maintained. For the case being considered here $L_d'\neq L_d$ so that a strained QW structure results.

The structure to be modeled consists of an $In_{0.53}Ga_{0.47}As$ layer sandwiched between thick InP barriers. After disordering, the concentration of the interdiffused atoms across the QW structure is assumed to have an error function distribution.[19] The constituent atom compositional profiles can, therefore, be represented as follows:

(i) in the group III sublattice, the In concentration after interdiffusion, $\tilde{x}(z)$, is described by

$$\tilde{x}(z)=1-\frac{1-x}{2}\left[\mathrm{erf}\left(\frac{L_z+2z}{4L_d}\right)+\mathrm{erf}\left(\frac{L_z-2z}{4L_d}\right)\right] \quad (1)$$

where L_z is the as-grown well width, z is the growth direction, and the QW is centered at $z=0$.

(ii) in the group V sublattice, the As compositional profile after interdiffusion, $\tilde{y}(z)$, is given by

$$\tilde{x}(z)=\frac{y}{2}\left[\mathrm{erf}\left(\frac{L_z+2z}{4L_d'}\right)+\mathrm{erf}\left(\frac{L_z-2z}{4L_d'}\right)\right] \quad (2)$$

where $y=1$ is the As concentration of the as-grown structure.

The compositional profiles in the disordered QW structure imply that the carrier effective mass, the bulk bandgap, the strain and its effects, if present, vary continuously across the QW. Consequently, the carrier effective mass, $m_r^*(z)$, is now z-dependent and is obtained from $m_r^*(z)=m_r^*(\tilde{x},\tilde{y})$, where $m_r^*(x,y)$ is the respective carrier $In_xGa_{1-x}As_yP_{1-y}$ bulk effective mass, and r denotes either the electron (C), heavy hole (V=HH), or light hole (V=LH). The unstrained (bulk) bandgap in the well, $E_g(\tilde{x},\tilde{y})$, is also a function of the compositional profile, so that the unstrained potential profile after interdiffusion, $\Delta E_r(\tilde{x},\tilde{y})$, varies across the well and is given by:

$$\Delta E_r(\tilde{x},\tilde{y})=Q_r\Delta E_g(\tilde{x},\tilde{y}) \quad (3)$$

where Q_r is the band offset and ΔE_g is the unstrained bandgap offset.

Since $L_d'\neq L_d$ a strained QW structure results after disordering. If the QW layer thickness is within the critical thickness regime, the QW structure will be coherently strained after disordering,[10] with a biaxial hydrostatic strain parallel to the interfacial plane and a uniaxial shear strain perpendicular to the interfacial plane. A compressive (tensile) hydrostatic strain causes an increase (decrease) in the bandgap energy by an amount determined by the hydrostatic deformation potential, defined as the shift in energy of the band edge per unit hydrostatic strain. The uniaxial (shear) strain disrupts the cubic symmetry of the semiconductor and lifts the degeneracy of the heavy hole (HH) and light hole (LH) band edges at the Brillouin zone centre Γ. The heavy hole band moves towards (away from) the conduction band and the light hole band moves away from (towards) the conduction band.[21] In addition, the presence of strain induces coupling between the LH valence band and the split-off band.[22]

The QW confinement potential profile after the disordering process, obtained by modifying the bulk postprocessing potential profile with the variable strain effects, is determined from[18]

$$U_r(z)=Q_r[\Delta E_g(\tilde{x},\tilde{y})-S_\perp(\tilde{x},\tilde{y})]\pm S_{/\!/r}(\tilde{x},\tilde{y}) \quad (4)$$

where $S_\perp(\tilde{x},\tilde{y})$ is the change in the bulk bandgap due to the biaxial component of strain, and $S_{/\!/r}(\tilde{x},\tilde{y})$ is the potential corresponding to the HH-LH band edge splitting induced by the uniaxial component of strain. $S_{/\!/HH}(\tilde{x},\tilde{y})$ and $S_{/\!/LH}(\tilde{x},\tilde{y})$ are asymmetric due to the coupling between the LH and split off band, and $S_{/\!/C}(\tilde{x},\tilde{y})=0$. The + sign in eq. (4) represents the confined HH profile, while the − sign represents the confined LH profile. The detailed expressions for $S_{/\!/HH}(\tilde{x},\tilde{y})$ and $S_{/\!/LH}(\tilde{x},\tilde{y})$ are derived in ref. 18.

The electron and hole subband structure at Γ can be calculated in the envelope function scheme[23] with the BenDaniel-Duke model[24] using a position dependent effective mass, by the one-dimensional Schrödinger-like equation expressed as

$$\frac{-\hbar^2}{2}\frac{\mathrm{d}}{\mathrm{d}z}\left[\frac{1}{m_r^*(z)}\frac{\mathrm{d}\chi_{rl}(z)}{\mathrm{d}z}\right]+U_r(z)\chi_{rl}(z)=E_{rl}\chi_{rl}(z) \quad (5)$$

where the growth direction z is the confinement axis, $\chi_{rl}(z)$ is the envelope wave function, E_{rl} is the quantized energy level with the subband energy zero at the bottom of the QW, and $l=p$ or q refers to the quantized subband energy levels for the electron and holes, respectively. This equation is solved numerically to obtain the quantized energy levels (E_{Cp}, E_{Vq}), and the envelope wave functions (χ_{Cp}, χ_{Vq}). A finite difference method is used, with the confinement profile defined in

eq. (4) and the boundary condition is taken to be zero at the end of the barrier ($\chi_{rl}(z_b) \simeq 0$, $z_b = 100$ nm).

The electron-heavy hole transition energy, $E_{CHH_{pq}}$, and the electron-light hole transition energy, $E_{CLH_{pq}}$, can then be obtained from

$$E_{CHH_{pq}} = E_{gHH}(\tilde{x}(0), \tilde{y}(0)) + E_{Cp} + E_{HHq} \quad (6.a)$$

$$E_{CLH_{pq}} = E_{gLH}(\tilde{x}(0), \tilde{y}(0)) + E_{Cp} + E_{LHq} \quad (6.b)$$

respectively, where $E_{gHH}(\tilde{x}(0), \tilde{y}(0))$ $E_{gLH}(\tilde{x}(0), \tilde{y}(0))$ are the electron-heavy hole and electron-light hole lowest direct bandgap at Γ after disordering, respectively.

3. Results and Discussion

The structure considered here is an undoped $In_{0.53}Ga_{0.47}As$ single QW layer, with an as-grown width $L_z = 6$ nm, lattice-matched to thick InP barriers. The effects of disordering are investigated by considering different rates of interdiffusion on the two sublattices. The parameter k is defined as $k = L_d'/L_d$ and results are presented for $0 \leq k \leq 6$. When $k < 1$ the interdiffusion rate on the group V sublattice is less than the interdiffusion rate on the group III sublattice, while for $k > 1$, the group V sublattice interdiffusion rate is larger than the group III sublattice one. The material parameters for the disordered structure are determined by interpolating between the binary parameters. Details of these parameters, and the bulk bandgap and the spin-orbit splitting compositional dependences, are given in ref. 18. A conduction band offset $Q_c = 60\%$ is used here.

The compositional profile, in-plane strain, and the carrier confinement potential for $L_d = 1$ nm and $L_d' = 0.25$ nm are shown in Fig. 1. In this case the interdiffusion takes place predominantly on the group III sublattice. In the early stages of the interdiffusion process, represented by $L_d \approx 1$ nm, the Ga atoms near the interface diffuse into the barrier, while In atoms diffuse into the well, but at the well center the Ga concentration hardly changes. Since $k = 0.25$ the As and P concentration profiles change very slowly and the interface is still quite abrupt. The increase in the In content in the well gives rise to a compressive strain in the disordered well. This compressive strain is largest near the interface and almost zero at the center, because of the In content profile across the well. The barrier close to the interface is practically InGaP, as can be seen from Fig. 1(a), and a tensile strain arises in the barrier near the interface since the InP lattice constant is always larger than that of InGaP. Thus the disordering process gives rise to the strain profile across the QW structure as shown in Fig. 1(b). This strain profile affects the shape and separation of the conduction and valence bands, and the HH and LH confinement potentials no longer coincide. The confinement profiles shown in Fig. 1(c) present interesting features at the top of the well, near the continuum, and at the bottom of the well, similar to the case of cation interdiffusion only.[18] A potential buildup occurs in the barrier near the interface because the bulk bandgap of InGaP is greater than that of InP.[25] However, this potential buildup is significantly

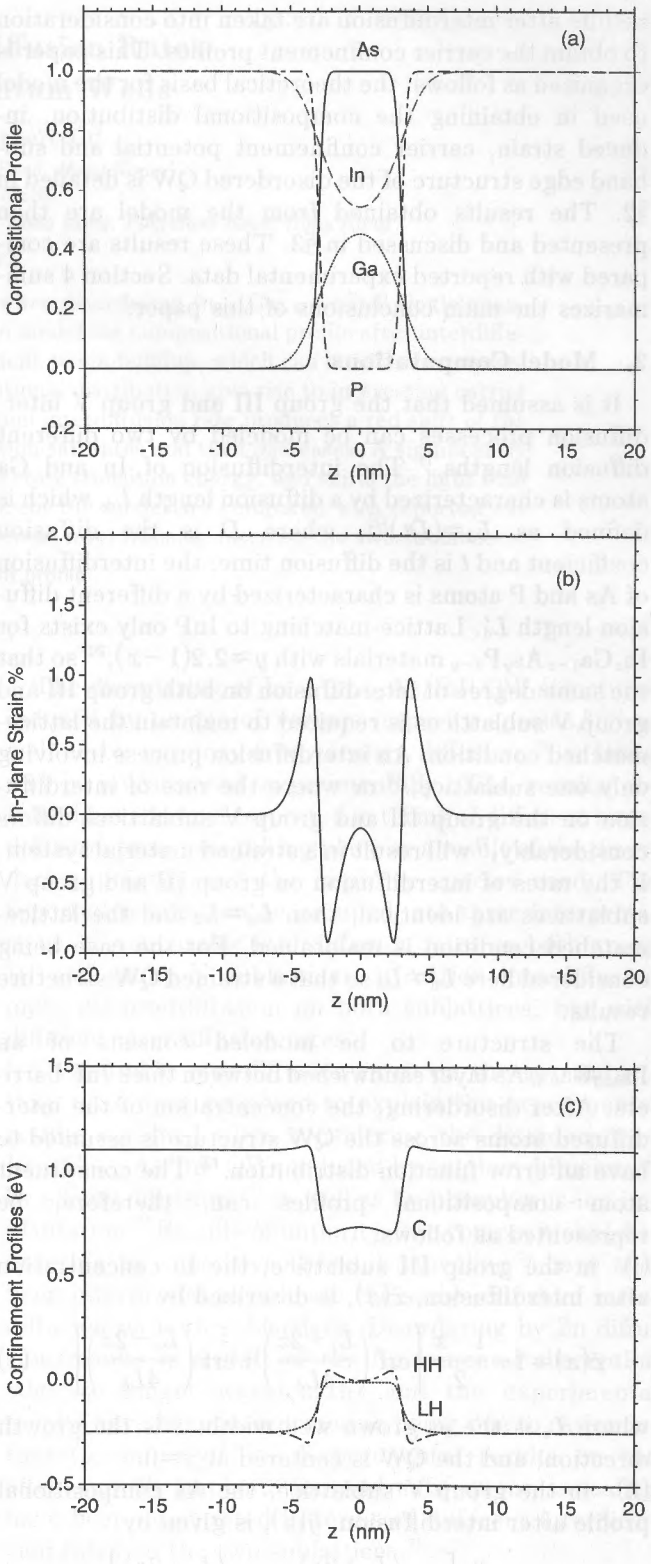

Fig. 1. Profiles of (a) composition, (b) in-plane strain, and (c) carrier confinement potential for $L_z = 6$ nm, $L_d = 1$ nm, $L_d' = 0.25$ nm, $Q_c = 60\%$, with well center at $z = 0$.

modified by the effects of the tensile strain in the barrier near the interface, and can even be reversed by strain, as can be seen for the LH confinement profile. Inside the well the bulk (unstrained) bandgap in the center of the well is larger than that at the interface, since the In content in the well center is less than that at the interface. The compressive strain is much smaller at

the well center so that the strain effects on the bandgap are much more pronounced at the interface. The combination of the bulk bandgap and the strain effects on this bandgap results in the potential at the well center being higher than that at the interface, giving rise to two miniwells.[17] The results obtained indicate that the HH subband ground state can be supported at energy levels that lie within the miniwells, while a quasi-bound state can result at an energy level corresponding to the potential buildup in the barrier near the interface.[18]

Figure 2 shows the compositional distribution, strain and confinement potential for the case $L_d=1$ nm, $L_d'=3$ nm. In this case interdiffusion on the group V sublattice is much faster than that on the group III sublattice. It can be seen from Fig. 2(a) that the well is now InGaAsP with the As and P concentrations almost at 50% at the well center. The InGaAsP profile across the well is such that a tensile strain is set up in the disordered well, as shown in Fig. 2(b). The compositional profile also causes a compressive strain in the barrier close to the interface. The combination of the unstrained bandgap and the effects of the strain profile on this bandgap gives rise to the confinement potentials shown in Fig. 2(c). The effects of the tensile strain, which now is at a maximum at the well center, are also clearly evident in the confinement potential. The tensile strain causes the LH potential profile to shift toward the electron (C) potential profile, while the HH potential profile is now shifted away from the C profile. Both the C and HH confinement profiles exhibit miniwells, while the LH confinement potential is a monotonically graded profile.

The effects of prolonged interdiffusion have also been investigated. The changes in the strain at the well center with interdiffusion duration, for various values of k, are shown in Fig. 3. $k=0$ represents cation interdiffusion only.[18] The compositional changes at the well center are insignificant in the early stages of interdiffusion ($L_d\approx1$ nm) so that the strain at the well center is very small. Subsequent interdiffusion, however, leads to a rapid reduction of the Ga concentration at the well center as the Ga atoms diffuse deeper into the barrier and tend toward a uniform distribution across the structure. The consequent increase in the In content results in a compressive strain at the well center, which increases with further interdiffusion. For $k=0.25$ and $k=0.5$, the strain at the well center is still compressive and large, as shown in Fig. 3. The rate of interdiffusion on the group III sublattice is significantly faster than that on the group V sublattice, and the InGaAsP composition in the well gives rise to the compressive strain. The lattice mismatch is now less than when $k=0$ (InGaAs well), and the compressive strain is thus smaller. In contrast with the case of cation interdiffusion only, the compressive strain at the well center for prolonged interdiffusion ($L_d\geq4$ nm) starts to decrease as a result of the now more pronounced effect of the competing, although slower, interdiffusion on the group V sublattice. When $k=1$ the InGaAsP well remains lattice-matched to the InP barrier so that there is no strain across the disordered QW structure.

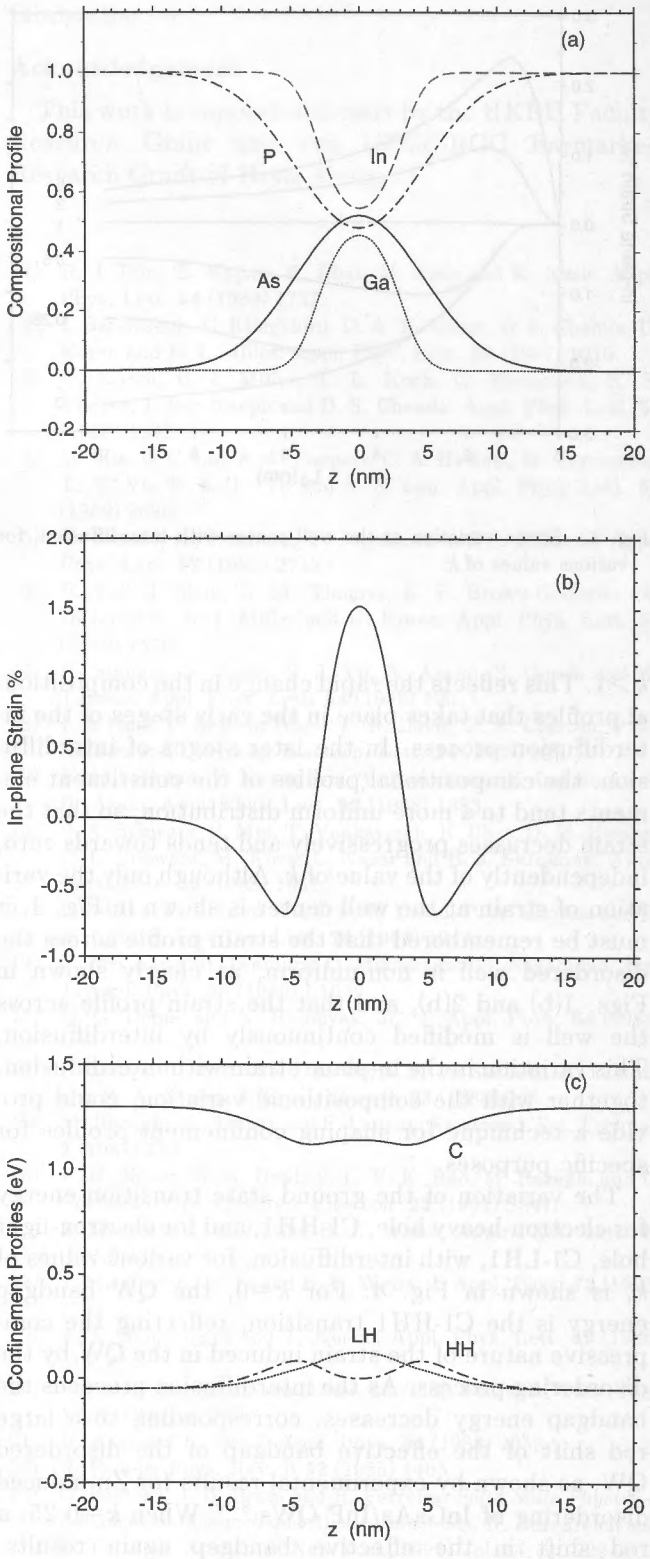

Fig. 2. Profiles of (a) composition, (b) in-plane strain, and (c) carrier confinement potential for $L_z=6$ nm, $L_d=1$ nm, $L_d'=3$ nm, $Q_c=60\%$, with well center at $z=0$.

For $k>1$ the rate of interdiffusion on the group V sublattice is higher than that on the group III sublattice. As already indicated, a tensile strain results at the well center. The larger the value of k, the higher is the tensile strain as a result of the increasing interdiffusion rate on the group V sublattice. The tensile strain at the well center peaks at around $L_d\approx1$ nm for values of

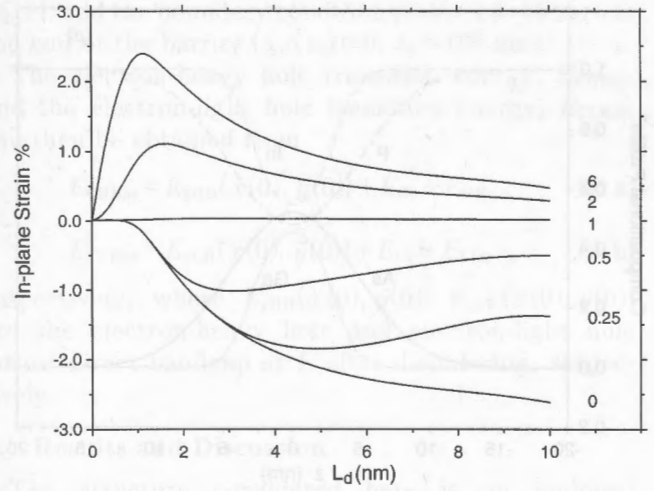

Fig. 3. Strain variation at the well center with interdiffusion, for various values of k.

$k>1$. This reflects the rapid change in the compositional profiles that takes place in the early stages of the interdiffusion process. In the later stages of interdiffusion, the compositional profiles of the constituent elements tend to a more uniform distribution, so that the strain decreases progressively and tends towards zero, independently of the value of k. Although only the variation of strain at the well center is shown in Fig. 3, it must be remembered that the strain profile across the disordered well is non-uniform, as clearly shown in Figs. 1(b) and 2(b), and that the strain profile across the well is modified continuously by interdiffusion. This variation in the in-plane strain with interdiffusion, together with the compositional variation, could provide a technique for shaping confinement profiles for specific purposes.

The variation of the ground state transition energy for electron-heavy hole, C1-HH1, and for electron-light hole, C1-LH1, with interdiffusion, for various values of k, is shown in Fig. 4. For $k=0$, the QW bandgap energy is the C1-HH1 transition, reflecting the compressive nature of the strain induced in the QW by the disordering process. As the interdiffusion proceeds the bandgap energy decreases, corresponding to a large red shift of the effective bandgap of the disordered QW, as shown by experimental results for Zn-induced disordering of InGaAs/InP QWs.[8-10] When $k=0.25$, a red shift in the effective bandgap again results. However, for long enough interdiffusion duration, the red shift saturates and even decreases. Some of the experimental results reported for Zn-induced disordering of InGaAs/InP QWs,[15,16] also show the red shift saturating and decreasing with increasing duration of the QW disordering process. The result obtained from our model is also similar to experimental results reported recently for disordering of GaInP/GaAs QWs by thermal annealing,[26] where the saturation and decrease of the red shift is interpreted as being due to the competing slower interdiffusion on the group V sublattice. For $k=0.5$, the red shift again saturates and then

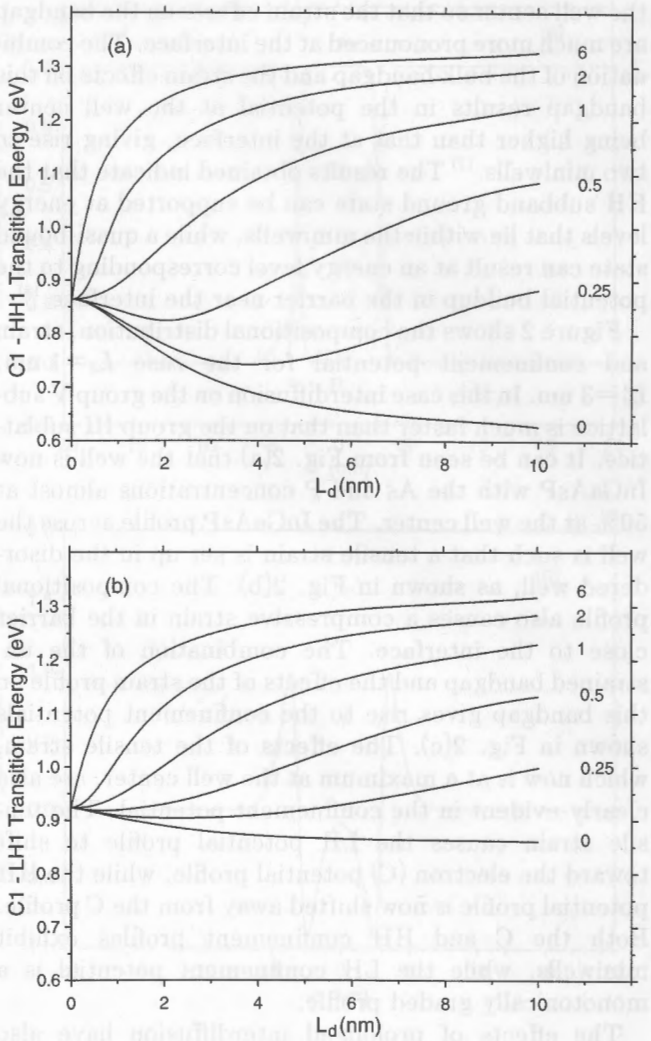

Fig. 4. Ground-state transition energy variation with interdiffusion, for various values of k, for (a) electron-heavy hole, and (b) electron-light hole.

decreases, but at an earlier stage of the interdiffusion process, since the competing group V sublattice interdiffusion is now more pronounced.

The ground state transition energy variation with interdiffusion for $k=1$ shows a blue shift in the effective bandgap of the disordered QW. This corresponds to experimental results for disordered InGaAs/InP using, for example, S diffusion.[11] The C1-HH1 transition energy is still smaller than the C1-LH1 transition energy, although as interdiffusion proceeds the two transition energies converge. Since the disordered structure in this case remains lattice-matched, the HH and LH confinement profiles coincide, and the difference between the two transition energies is simply a result of the different quantization effects for the HH and LH due to their different effective masses. Since the effective well width increases as interdiffusion proceeds,[27] the difference in the quantization effects for the HH and LH decreases, and the transition energies converge.

A blue shift is also obtained when $k>1$. In the early stages of interdiffusion, this shift is significantly larger when compared with the results obtained for $k<1$. For

instance, the change in the C1-HH1 transition energy for $k=2$ in going from $L_d=0$ to 2 nm corresponds to a shift to shorter wavelengths of about 300 nm, from about 1.4 to 1.1 μm. The corresponding change in the C1-HH1 transition energy for $k=0.5$ represents a shift to longer wavelengths of about 100 nm, from about 1.4 to 1.5 μm. The change from a ternary to a quaternary QW is more rapid when the group V sublattice interdiffusion predominates since the group V atoms composition across the as-grown QW structure is 100% As in the well and 100% P in the barrier. Comparison of Figs. 4(a) and 4(b) shows that when $k>1$, the C1-LH1 transition energy becomes smaller than the C1-HH1 transition energy. This is due to the fact that the QW is now under tensile strain. The results shown indicate that the LH ground state is effectively shifted above the HH ground state. This is of considerable interest for applications such as semiconductor lasers where the significantly lower effective mass of the light holes approaches better the ideal requirement of equal conduction and valence band masses.[28] Optimization of the disordering process could thus induce a tensile strain that could be used to obtain desired valence band splitting effects useful in specific photonic applications.

4. Conclusions

The disordering of $In_{0.53}Ga_{0.47}As/InP$ QWs has been modeled considering different interdiffusion rates on the group III and group V sublattices. An error function distribution is used to represent the constituent atoms composition after disordering. A strained QW structure results after disordering and the effects of the strain profile together with the unstrained bandgap profile due to the compositional distribution give rise to carrier confinement potentials that exhibit distinctive characteristics which could be of use in photonic applications.

When the cation interdiffusion rate is faster than the anion interdiffusion rate the ground-state (C1-HH1) transition shifts to longer wavelengths. The results from the model show that for prolonged interdiffusion this shift to longer wavelengths saturates and then decreases. This is in agreement with reported experimental results of Zn-induced disordering of $In_{0.53}Ga_{0.47}As/InP$ QWs, as well as of thermal annealing of GaInP/GaAs QWs. When the anion interdiffusion is faster than the cation interdiffusion, the results show that the effective bandgap of the disordered QW would be the C1-LH1 ground-state transition, which shifts to shorter wavelengths with interdiffusion. The tensile strain that is induced under these disordering conditions shifts the LH ground state above the HH ground state. This result could be of interest in laser applications. The results presented here show that the control of the relative extent of cation and anion interdiffusion offers interesting possibilities for optoelectronic device fabrication.

Acknowledgement

This work is supported in part by the HKBU Faculty Research Grant and the UPGC-RGC Earmarked Research Grant of Hong Kong.

1) R. J. Deri, E. Kapon, R. Bhat, M. Seto and K. Kash: Appl. Phys. Lett. **54** (1989) 1737.
2) I. Bar-Joseph, C. Klingshirn, D. A. B. Miller, D. S. Chemla, U. Koren and B. I. Miller: Appl. Phys. Lett. **50** (1987) 1010.
3) U. Koren, B. I. Miller, T. L. Koch, G. Eisenstein, R. S. Tucker, I. Bar-Joseph and D. S. Chemla: Appl. Phys. Lett. **51** (1987) 1132.
4) W. Xia, S. C. Lin, S. A. Pappert, C. A. Hewett, M. Fernandes, T. T. Vu, P. K. L. Yu and S. S. Lau: Appl. Phys. Lett. **55** (1989) 2020.
5) Y. Suzuki, H. Iwamura, T. Miyazawa and O. Mikami: Appl. Phys. Lett. **57** (1990) 2745.
6) B. Tell, J. Shah, D. M. Thomas, K. F. Brown-Goebeler, A. DiGiovanni, B. I. Miller and U. Koren: Appl. Phys. Lett. **54** (1989) 1570.
7) H. Sumida, H. Asahi, S. J. Yu, K. Asami, S. Gonda and H. Tanoue: Appl. Phys. Lett. **54** (1989) 520.
8) I. J. Pape, P. Li Kam Wa, J. P. R. David, P. A. Claxton, P. N. Robson and D. Sykes: Electron. Lett. **24** (1988) 910.
9) K. Nakashima, Y. Kawaguchi, Y. Kawamura, Y. Imamura and H. Asahi: Appl. Phys. Lett. **52** (1988) 1383.
10) S. A. Schwarz, P. Mei, T. Venkatesen, R. Bhat, D. M. Hwang, C. L. Schwarz, M. Koza, L. Nazar and B. J. Skromme: Appl. Phys. Lett. **53** (1988) 1051.
11) I. J. Pape, P. Li Kam Wa, J. P. R. David, P. A. Claxton and P. N. Robson: Electron. Lett. **24** (1988) 1217.
12) T. Miyazawa, H. Iwamura, O. Mikami and M. Naganuma: Jpn. J. Appl. Phys. **28** (1989) L1039.
13) D. G. Deppe and N. Holonyak, Jr.: J. Appl. Phys. **64** (1988) R93.
14) F. Iikawa, P. Motisuke, J. A. Brum, M. A. Sacilotti, A. P. Roth and R. A. Masut: J. Cryst. Growth **93** (1988) 336.
15) M. Razeghi, O. Archer and F. Launay: Semicond. Sci. Technol. **2** (1987) 793.
16) F. H. Julien, M. A. Bradley, E. V. K. Rao, M. Razeghi and L. Goldstein: Opt. Quantum Electron. **23** (1991) S847.
17) J. Micallef, E. H. Li and B. L. Weiss: Appl. Phys. Lett. **61** (1992) 435.
18) J. Micallef, E. H. Li and B. L. Weiss: J. Appl. Phys. **73** (1993) 7524.
19) T. E. Schlesinger and T. Kuech: Appl. Phys. Lett. **49** (1986) 519.
20) *GaInAsP Alloy Semiconductors*, ed. T. P. Pearsall (Wiley, New York, 1982) p. 295.
21) H. Asai and K. Oe: J. Appl. Phys. **54** (1983) 2052.
22) R. People: Phys. Rev. B **32** (1985) 1405.
23) G. Bastard, J. B. Brum and R. Ferreira: *Solid State Physics—Advances in Research and Applications*, eds. H. Ehrenreich and D. Turnbull (Academic, New York, 1991) Vol. 44, pp. 229–415.
24) D. J. BenDaniel and C. B. Duke: Phys. Rev. **152** (1966) 683.
25) S. Adachi: J. Appl. Phys. **53** (1982) 8775.
26) C. Francis, M. A. Bradley, P. Boucaud, F. H. Julien and M. Razeghi: Appl. Phys. Lett. **62** (1993) 178.
27) E. H. Li, J. Micallef and B. L. Weiss: Jpn. J. Appl. Phys. **31** (1992) L7.
28) E. Yablonovich and E. O. Kane: J. Lightwave Technol. **6** (1988) 1292.